ADVANCED HEALTHCARE MATERIALS
www.advhealthmat.de

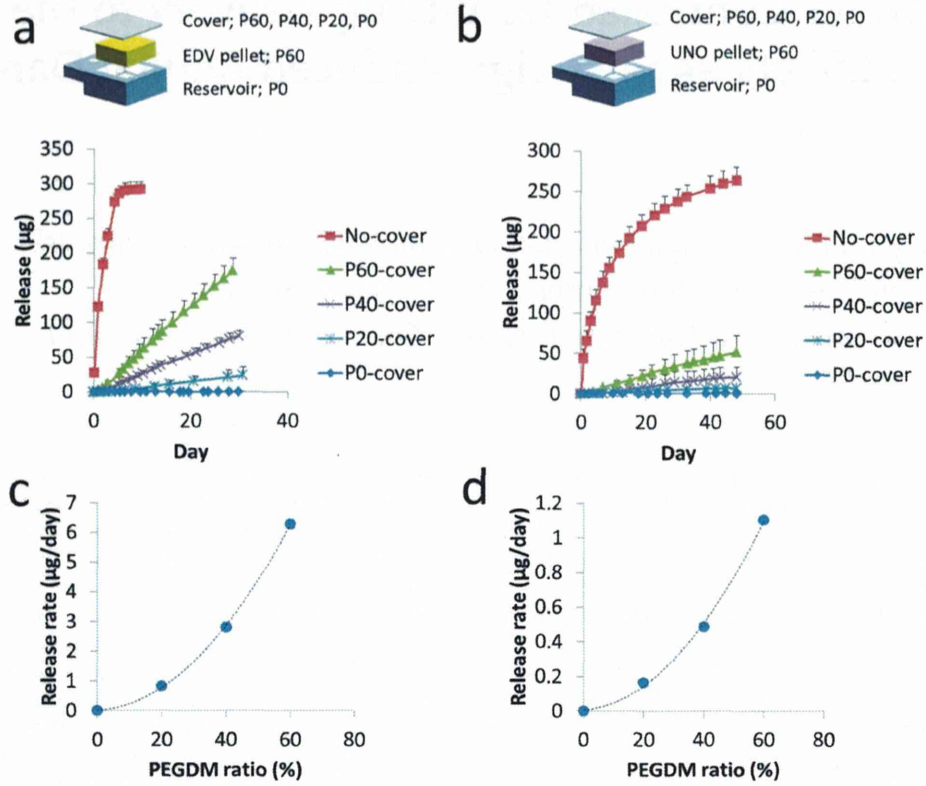

Figure 1. Release of a) EDV and b) UNO from devices sealed with various PEGDM/TEGDM covers. Correlation between PEGDM ratio in the cover and release rate of c) EDV and d) UNO. Release rate was estimated from the slope of the curve at the initial stable release period in (a) and (b). Values are mean ± SD.

through the cover. The release rate may be influenced by physical characteristics of the drug substance such as lipophilicity and water solubility.[18] In fact, hydrophobic UNO exhibited a lower release rate than hydrophilic EDV under the same device conditions (Figure 1).

The dual-drug release device was next applied to a light-induced retinal injury model and retinal function was evaluated using an electroretinogram (ERG) and compared to results obtained using single-drug release devices. The devices are designed for implantation on the rat sclera and they release drugs unidirectionally via a cover to the scleral side by encapsulating drugs with a TEGDM (P0) reservoir (**Figure 2**a). To evaluate the effects of the EDV/UNO-loaded device, PBS/PBS-, EDV/PBS-, UNO/PBS-, and EDV/UNO-loaded devices were fabricated as shown in Figure 2b. The appropriate combination of EDV- and UNO-formulations was evaluated using P40 and P60. The combination of EDV in P60 (E60)/UNO in P40 (U40) showed more effective protection as a function of ERG amplitudes than the other combinations of E60/UNO in P60 (U60), EDV in P40 (E40)/U60, and E40/U40 (Figure S1, Supporting Information). Therefore, an E60/U40 (EDV/UNO)-loaded device (Figure 2c) that could release EDV and UNO at concentrations of 3.24 and 0.79 µg per day, respectively (Figure 2d), was used to evaluate the effects of co-delivery of EDV and UNO via this device. The EDV/UNO-loaded device demonstrated higher ERG amplitudes than the single-drug-loaded devices and the PBS-loaded device (Figure 2e). Although single-drug administrations showed significantly higher amplitudes compared with the PBS-loaded device, multiple administrations resulted in b-waves having significantly higher amplitudes compared to those elicited by single administrations of EDV and UNO (Figure 2f,g).

Histological evaluation revealed that the outer nuclear layer (ONL) thickness was preserved in the transplanted superior retina in all of the drug-loaded device groups, in contrast to the PBS-device group (**Figure 3**a), and many points of the inferior retina through the phase of the optic disc were also preserved in the EDV/UNO-loaded device group (Figure 3b). TUNEL (Figure 3c) and quantitative analysis were used to study light-induced apoptotic cell death, and they indicated that the EDV/UNO-loaded device significantly reduced the number of TUNEL-positive cells compared with single-drug-loaded devices (Figure 3d). Western blots were performed 15 d after light injury (11 d after ERG), because phosphorylated p38 (p-p38) increased 15 d after light injury (Figure S2, Supporting Information). P-p38 was decreased in the drug-loaded device groups compared with the PBS-loaded device group and it was lowest in the EDV/UNO-loaded device group (Figure 3e). Statistically significant lower levels of p-p38 were observed in the EDV/UNO device group compared to the PBS-loaded device group. On the other hand, phosphorylated ERK1/2 (p-ERK1/2) was found to be lowest in the PBS-loaded device group, while it increased in the drug-loaded device groups and was highest in the EDV/UNO-loaded device group (Figure 3f). Statistically

DOI: 10.1002/adhm.201400114

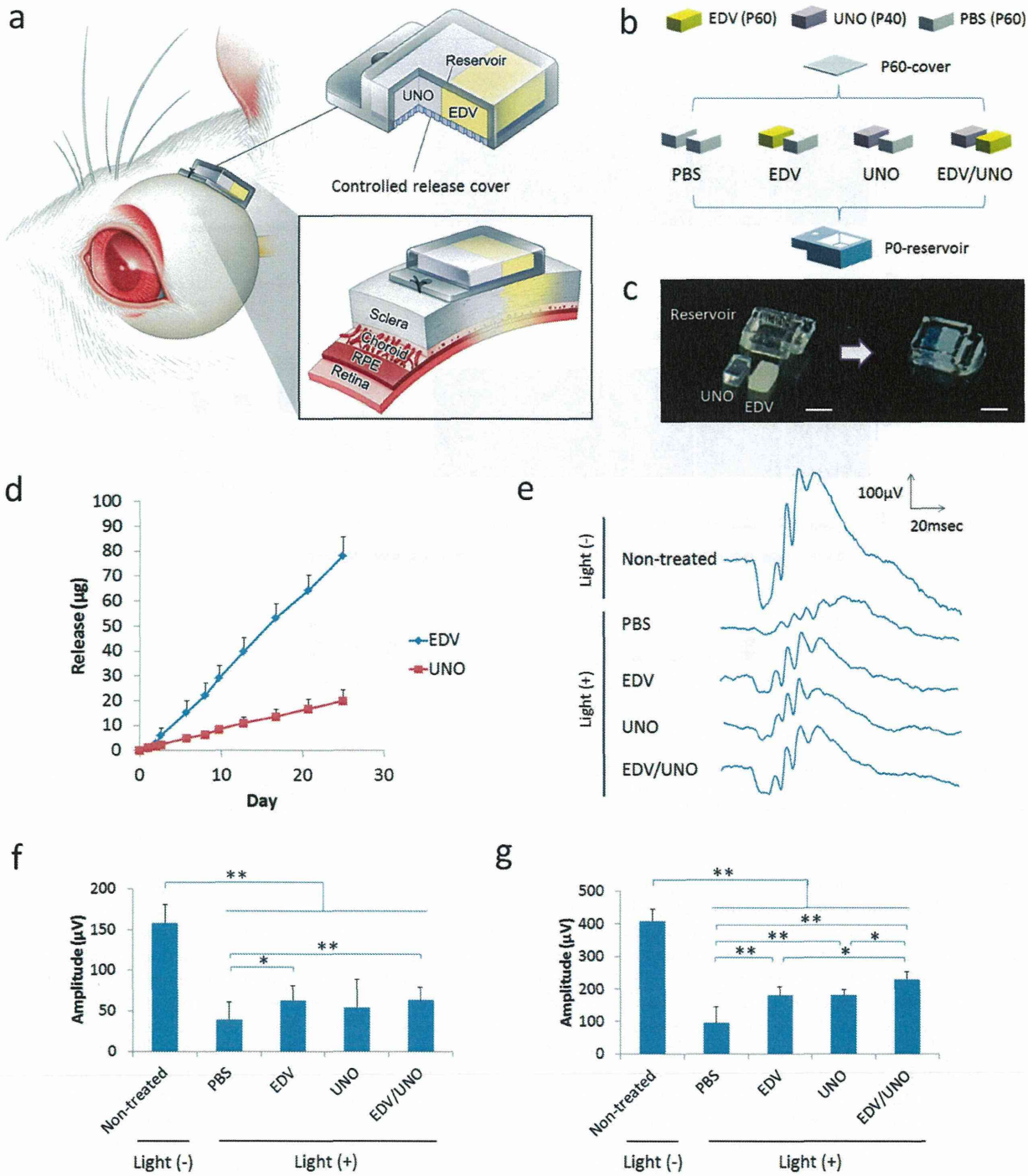

Figure 2. a) Schematic image of the device implantation on the rat sclera. b) Device conditions for in vivo study of synergistic protective effects of EDV and UNO. c) Photographs showing two kinds of pellets, including UNO and EDV, and a reservoir before assembling, and the device after assembling. d) Simultaneous in vitro release profiles of EDV and UNO from the device that combined EDV pelletized with P60 and UNO pelletized with P40, and covered with P60. Representative ERG spectra after light injury in rats e) and ERG amplitudes of a–f) and b-waves g) in the EDV/UNO-loaded device-treated group (EDV/UNO), the EDV/PBS-loaded device-treated group (EDV), the UNO/PBS-loaded device-treated group (UNO), and the PBS/PBS-loaded device-treated group (PBS). Values are mean ± SD. $^{*}P < 0.05$, $^{**}P < 0.01$ (one-way analysis of variance (ANOVA) with Tukey's test).

significant higher p-ERK1/2 expression was observed in the EDV/UNO-loaded device group compared to that of the PBS-loaded device group.

In the in vivo experiments, reduction of ONL thickness, expression of TUNEL-positive cells, and reduction of ERG amplitudes after light exposure were precluded in groups

ADVANCED HEALTHCARE MATERIALS
www.advhealthmat.de

www.MaterialsViews.com

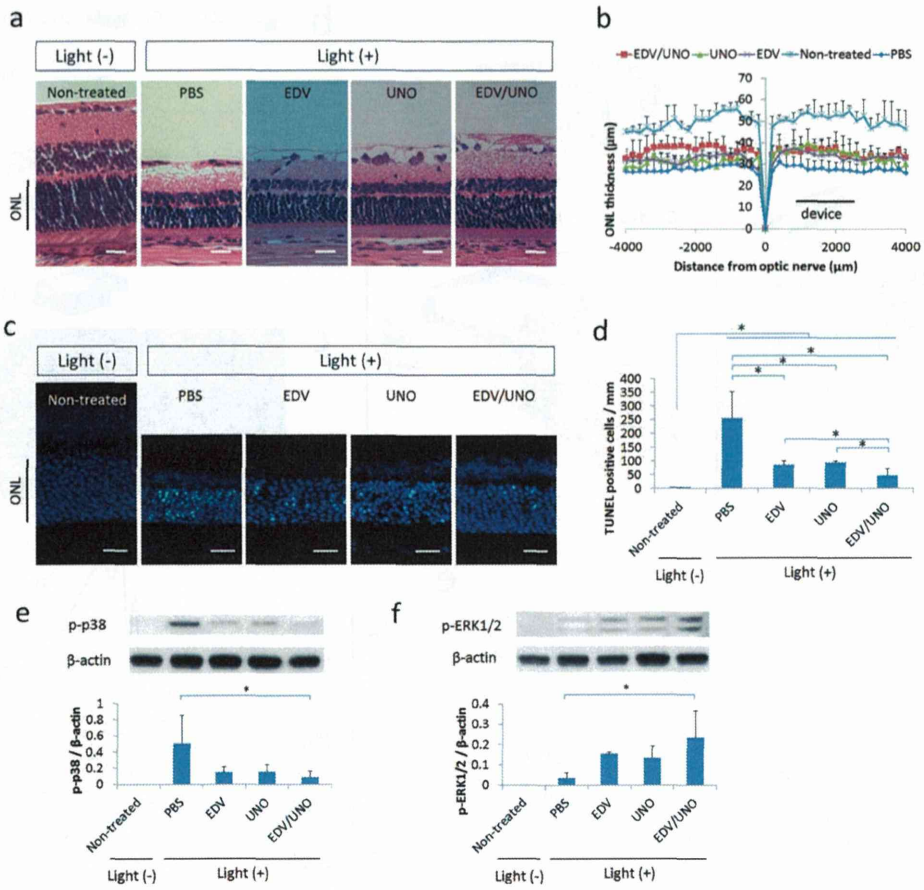

Figure 3. a) Retinal cross-sections, b) ONL thickness, c) TUNEL staining, d) TUNEL-positive cell number and western blotting for e) phosphorylated p-38 and f) ERK1/2 of retinal specimens from rats treated with PBS/PBS-, EDV/PBS-, UNO/PBS-, and EDV/UNO-loaded devices 15 d after light exposure. Scale bars; 20 μm. Values are mean ± SD. $*P < 0.05$, $**P < 0.01$ (one-way analysis of variance (ANOVA) with Tukey's test).

treated with EDV/UNO-loaded devices, suggesting that co-delivery of EDV and UNO attenuates light-induced retinal damage both morphologically and functionally. The cyto-protective actions of EDV and UNO that were observed in the in vitro cell culture experiments (Figure S3, Supporting Information) might correlate with retinal neuroprotection. EDV could reduce oxidative damage by suppressing ROS generation,[11] which in turn would attenuate the increase of $[Ca^{2+}]_i$ as seen in the in vitro cell culture results (Figure S4, Supporting Information). UNO could prevent the intracellular Ca^{2+} increase,[12,13] resulting in an anti-apoptotic effect (Figure S5, Supporting Information). ROS leads to the activation of MAP kinase signaling, including p38 and ERK1/2, elevates cellular Ca^{2+} levels, and induces oxidative damage.[19] Thus, down-regulation of p-p38 by suppressing ROS generation might correlate with the rescue of the cells from apoptosis (Figure 3e).[20,21] ERK1/2 activation may act in some cases to promote cell survival while also participating in pathways leading to neuronal cell death.[22] Although the exact role of ERK1/2 after light injury is unclear, up-regulation of p-ERK1/2 by drug administrations might correlate with cell survival (Figure 3f).

Strict local delivery of the drugs through the device described herein would avoid the risk of side effects from systematic application. Additionally, prolonged sustained drug release would be suitable in treating chronic retinal diseases. Previous studies reporting multiple drug delivery systems, however, did not address independent release control and had a short drug release period.[23] Furthermore, release profiles for biodegradable systems are generally complex, and they may have associated burst effects.[24] In contrast, a non-biodegradable device containing a drug reservoir sealed with a controlled release cover allows for sustained release and reduces the sizes of the bursts.[25–28] It is theoretically possible that the device utilized for these experiments in a rat model system could effectively release EDV and UNO for 46 and 188 d, respectively (Figure 2d). In spite of the promising carriers reported previously, in vivo evidence for the potential of multi-drug delivery has not yet been provided to date. Consequently, to the best of our knowledge, we are the first to demonstrate evidence for retinal neuroprotective effects of controlled transscleral co-delivery of EDV and UNO in a retinal degeneration model.

Comparable studies using larger animals are planned to investigate differences in drug permeability and efficacy among

DOI: 10.1002/adhm.201400114

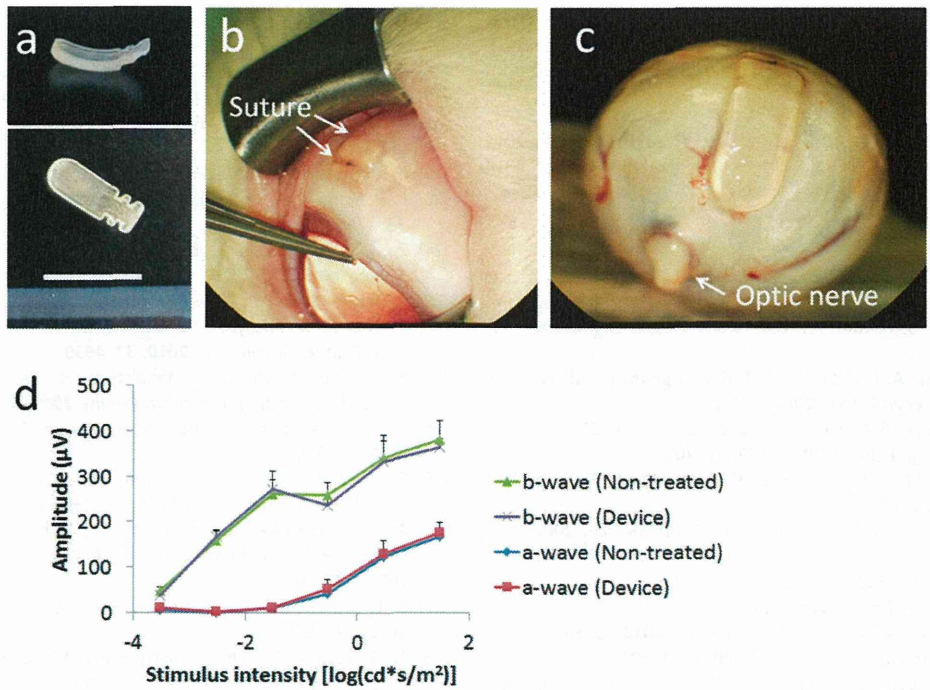

Figure 4. a) Prototype of the device used in the rabbit experiments. This device has a rounded shape that fits on the rabbit eyeball and is thin (thickness; 1.6 mm) to avoid discomfort after implantation. The reservoir has dimples to fix it on the sclera by suture, shown as arrows in b). c) The device, which has the reservoir located at one end, was placed so that the reservoir reached the posterior site near the optic nerve. d) ERG amplitudes 8 weeks after implantation. Scale bar: 10 mm. Values are mean ± SD.

different species using a prototype device designed for a rabbit model (**Figure 4**a). The device materials, PEGDM and TEGDM, can be easily molded into different substrate shapes by UV curing.[29,30] A microfabrication technique was used because the shape and volume of the reservoir can be easily modified by AutoCAD design (Figure S6, Supporting Information). The device has grooves for suture to fix it on the sclera (Figure 4b), and it is designed to fit the curve of the eyeball. The edge, where the drug reservoir is located, of the device could reach around the posterior segment of the eye, especially the macular area in the case of humans (Figure 4c). There was no difference in ERG amplitudes from device-implanted eyes versus non-treated eyes 8 weeks after implantation (Figure 4d), suggesting that the device could be used to safely administer drugs by the transscleral approach without disturbing intraocular tissues.

One of the limitations of this study is the lack of a specific stochastic search for drugs. Although EDV and UNO were selected based on previous reports of their neuroprotective effects against light-induced retinal damage following systemic administration,[10,11] many drug search algorithms have been used to select drug numbers and/or concentrations for multi-drug applications.[31,32] The limited span of the in vivo experiments, due to the study design (24 d from implantation to sacrifice), means that the duration of the effect and the appearance of side effects after long-term drug delivery remain to be determined.

In conclusion, a polymeric system that can simultaneously administer two drugs having distinct kinetics showed synergistic retinal neuroprotection against light injury in rats when compared with single-drug-loaded devices. The device can be designed to contain various drug formulations and dosages, and it can be microfabricated as various forms for implantation on the sclera of rats, rabbits, and potentially humans, allowing for a wide range of potential biomedical applications. Transscleral administration by our device would offer a safer therapeutic method than intravitreal injections or intraocular implants. Thus, our device is expected to be a promising candidate for sustained intraocular multi-drug delivery.

Experimental Section

Experimental details are described in the Supporting Information.

Supporting Information

Supporting Information is available from the Wiley Online Library or from the author.

Acknowledgements

The authors thank E. Koyanagi for help with HPLC. The authors also thank T. Kawashima, N. Kumasaka, and T. Yamada for help with device molds preparation. This study was supported by a Grant-in-Aid for Young Scientists (A) from the Ministry of Education, Culture, Sports, Science, and Technology (No. 23680054), and a Health Labour Sciences

ADVANCED HEALTHCARE MATERIALS
www.advhealthmat.de

www.MaterialsViews.com

Research Grant from the Ministry of Health Labour and Welfare (H23-iryokiki-wakate-003, H23-kankaku-ippan-004, H24-nanchitoh-ippan-067). Based on the collaborative research agreement, UNO is provided from R-tech Ueno, to which Y.M. belongs.

Received: February 24, 2014
Revised: March 26, 2014
Published online:

[1] S. Resnikoff, D. Pascolini, D. Etya'ale, I. Kocur, R. Pararajasegaram, G. P. Pokharel, S. P. Mariotti, *Bull. World Health Organ* **2004**, *82*, 844.
[2] E. S. Gragoudas, A. P. Adamis, E. T. Cunningham Jr., M. Feinsod, D. R. Guyer, *N. Engl. J. Med.* **2004**, *351*, 2805.
[3] M. Kim, B. J. Yoon, *BMC Genomics* **2012**, *13*, Suppl 6, S12.
[4] D. J. Calkins, *Prog. Retin Eye Res.* **2012**, *31*, 702.
[5] Q. L. Fu, X. Li, H. K. Yip, Z. Shao, W. Wu, S. Mi, K. F. So, *Neuroscience* **2009**, *162*, 375.
[6] D. H. Shin, R. M. Feldman, W. P. Sheu, *Ophthalmology* **2004**, *111*, 276.
[7] R. F. Spaide, *Retina* **2009**, *29*, S5.
[8] M. P. Murphy, *Sci. Signal* **2012**, *5*, pe39.
[9] Y. X. Wang, Y. M. Zheng, *Antioxid Redox Signal* **2010**, *12*, 611.
[10] K. Hayami, K. Unoki, *Ophthalmic Res.* **2001**, *33*, 203.
[11] S. Imai, Y. Inokuchi, S. Nakamura, K. Tsuruma, M. Shimazawa, H. Hara, *Eur. J. Pharmacol.* **2010**, *642*, 77.
[12] K. Tsuruma, Y. Tanaka, M. Shimazawa, Y. Mashima, H. Hara, *Mol. Vis.* **2011**, *17*, 3556.
[13] J. Cuppoletti, D. H. Malinowska, K. P. Tewari, J. Chakrabarti, R. Ueno, *Biochim. Biophys. Acta* **2007**, *1768*, 1083.
[14] N. Nagai, H. Kaji, H. Onami, Y. Ishikawa, M. Nishizawa, N. Osumi, T. Nakazawa, T. Abe, *Acta Biomater.* **2014**, *10*, 680.
[15] D. H. Geroski, H. F. Edelhauser, *Adv. Drug Delivery Rev.* **2001**, *52*, 37.
[16] V. P. Ranta, A. Urtti, *Adv. Drug Delivery Rev.* **2006**, *58*, 1164.
[17] J. Ambati, A. P. Adamis, *Prog. Retin Eye Res.* **2002**, *21*, 145.
[18] S. H. Dickens, G. M. Flaim, C. J. Floyd, *Dent Mater.* **2010**, *26*, 675.
[19] H. Kamata, H. Hirata, *Cell Signal* **1999**, *11*, 1.
[20] L. P. Yang, X. A. Zhu, M. O. Tso, *Invest Ophthalmol. Vis. Sci.* **2007**, *48*, 4766.
[21] Z. Xia, M. Dickens, J. Raingeaud, R. J. Davis, M. E. Greenberg, *Science* **1995**, *270*, 1326.
[22] Y. Luo, D. B. DeFranco, *J. Biol. Chem.* **2006**, *281*, 16436.
[23] R. Elia, P. W. Fuegy, A. VanDelden, M. A. Firpo, G. D. Prestwich, R. A. Peattie, *Biomaterials* **2010**, *31*, 4630.
[24] N. Kunou, Y. Ogura, T. Yasukawa, H. Kimura, H. Miyamoto, Y. Honda, Y. Ikada, *J. Controlled Release* **2000**, *68*, 263.
[25] D. A. Bernards, K. D. Lance, N. A. Ciaccio, T. A. Desai, *Nano Lett.* **2012**, *12*, 5355.
[26] S. Ferrati, D. Fine, J. You, E. De Rosa, L. Hudson, E. Zabre, S. Hosali, L. Zhang, C. Hickman, S. Sunder Bansal, A. M. Cordero-Reyes, T. Geninatti, J. Sih, R. Goodall, G. Palapattu, M. Kloc, R. M. Ghobrial, M. Ferrari, A. Grattoni, *J. Controlled Release* **2013**, *172*, 1011.
[27] C. L. Stevenson, J. T. Santini, Jr., R. Langer, *Adv. Drug Delivery Rev.* **2012**, *64*, 1590.
[28] N. A. Peppas, *Adv. Drug Delivery Rev.* **2013**, *65*, 5.
[29] D. S. Benoit, A. R. Durney, K. S. Anseth, *Tissue Eng.* **2006**, *12*, 1663.
[30] S. Kalachandra, *Dent Mater.* **1989**, *5*, 283.
[31] D. Calzolari, S. Bruschi, L. Coquin, J. Schofield, J. D. Feala, J. C. Reed, A. D. McCulloch, G. Paternostro, *PLoS Comput. Biol.* **2008**, *4*, e1000249.
[32] P. K. Wong, F. Yu, A. Shahangian, G. Cheng, R. Sun, C. M. Ho, *Proc. Natl. Acad. Sci. U.S.A.* **2008**, *105*, 5105.

Acta Biomaterialia 10 (2014) 680–687

Contents lists available at ScienceDirect

Acta Biomaterialia

journal homepage: www.elsevier.com/locate/actabiomat

A polymeric device for controlled transscleral multi-drug delivery to the posterior segment of the eye

Nobuhiro Nagai [a], Hirokazu Kaji [b], Hideyuki Onami [a,c], Yumi Ishikawa [a], Matsuhiko Nishizawa [b], Noriko Osumi [d], Toru Nakazawa [c], Toshiaki Abe [a,*]

[a] Division of Clinical Cell Therapy, United Centers for Advanced Research and Translational Medicine (ART), Tohoku University Graduate School of Medicine, 2-1 Seiryo-machi, Aoba-ku, Sendai 980-8575, Japan
[b] Department of Bioengineering and Robotics, Graduate School of Engineering, Tohoku University, 6-6-01 Aramaki, Aoba-ku, Sendai 980-8579, Japan
[c] Department of Ophthalmology, Tohoku University Graduate School of Medicine, 1-1 Seiryo-machi, Aoba-ku, Sendai 980-8574, Japan
[d] Division of Developmental Neuroscience, United Centers for Advanced Research and Translational Medicine (ART), Tohoku University Graduate School of Medicine, 2-1 Seiryo-machi, Aoba-ku, Sendai 980-8575, Japan

ARTICLE INFO

Article history:
Received 28 August 2013
Received in revised form 26 October 2013
Accepted 8 November 2013
Available online 15 November 2013

Keywords:
Transscleral delivery
Multi-drug delivery
Retina
Poly(ethyleneglycol) dimethacrylate

ABSTRACT

The design of drug delivery systems that can deliver multiple drugs to the posterior segment of the eye is a challenging task in retinal disease treatments. We report a polymeric device for multi-drug transscleral delivery at independently controlled release rates. The device comprises a microfabricated reservoir, controlled-release cover and three different fluorescent formulations, which were made of photopolymeized tri(ethyleneglycol)dimethacrylate (TEGDM) and poly(ethyleneglycol)dimethacrylate (PEGDM). The release rate of each fluorescent is controlled by varying the PEGDM/TEGDM ratio in its formulation and the cover. The release kinetics appeared to be related to the swelling ratio of the PEGDM/TEGDM polymers. When the devices were implanted onto rat sclerae, fluorescence was observable in the ocular tissues during 4 weeks' implantation and distributed locally around the implantation site. Our polymeric system, which can administer multiple compounds with distinct kinetics, provides prolonged action and less invasive transscleral administration, and is expected to provide new tools for the treatment of posterior eye diseases with new therapeutic modalities.

1. Introduction

Diseases of the posterior eye segments cause impaired vision and blindness for millions of patients around the world [1]. There has been an increase in the understanding of the disease processes, and multiple factors have been reported to play a role in the diseases [2–4]. Thus, multi-drug therapy has become the primary method of disease management, because it offers the major advantages of enhanced efficacy of treatment, reduction of each drug dose, and mitigation of toxicity and side-effects caused by high doses of single drugs [5–7]. Multiple drugs have been used to treat patients with glaucoma [5,6] and to suppress choroidal neovascularization in patients with age-related macular degeneration (AMD) [7]. The regulation of neovascularization has received much attention, and it is now known that its balance is maintained by more than two dozen cytokines [8]. Thus it would be more effective and reasonable to use a number of drugs to treat such disease processes. Some techniques and novel pharmacological agents offer promise for the future treatment of posterior eye segment diseases [9–11]. However, the successful treatment of some retinal diseases has been limited. The limitation may be partially related to inadequate drug delivery systems for the retina, including multiple drug administration.

The principal route for local ophthalmic drug delivery remains topical application [12]. However, drug delivery to intraocular tissue by this approach is limited by the significant barrier of corneal epithelium and tear fluid turnover [13]. Systemic drug administration is not a viable alternative due to the blood–retinal barrier that limits drug access to the posterior tissues of the eye. Although intravitreal injections and intraocular implants may deliver drugs effectively to the retina and choroid, this approach is invasive to the eye and may cause severe adverse effects, such as endophthalmitis and retinal detachment [14]. Periocular or transscleral routes are less invasive than intravitreal administration and provide higher retinal and vitreal drug bioavailability (~0.01–0.1%) compared to eye drops (about 0.001% or less) [15,16]. Due to the high degree of hydration and low cell density of the sclera, soluble substrates readily pass through the sclera, although the ease of penetration of the drug to the vitreous cavity is dependent on the thickness

* Corresponding author. Tel./fax: +81 22 717 8234.
E-mail address: toshi@oph.med.tohoku.ac.jp (T. Abe).

1742-7061/$ - see front matter © 2013 Acta Materialia Inc. Published by Elsevier Ltd. All rights reserved.
http://dx.doi.org/10.1016/j.actbio.2013.11.004

of the sclera [17]. Thus transscleral delivery has the potential to be a more effective and less invasive route for intraocular drug delivery.

Several potential carriers for ocular drug delivery such as micelles [18], microneedles [19], nano- or microparticles [20,21], liposomes [22,23] and hydrogel systems [24,25] have been investigated. All the systems are injectable for localized and targeted delivery of drugs to the desired site and biodegradable to avoid a second procedure for implant removal. However, release profiles for biodegradable systems are generally complex with burst effects, i.e. an initial burst, a diffusional release phase and a final burst [26]. Additionally, the release period of such biodegradable systems is limited to less than 2 weeks [25]. In chronic eye diseases such as AMD and retinitis pigmentosa, duration of effect with controlled drug release is critical. Although several systems for multi-drug delivery have been developed [27–32], there are none intended for ocular multi-drug delivery.

In this work, we manufactured a polymeric device for multi-drug transscleral delivery to the posterior segment of the eye at independently controlled release rates (Fig. 1). The device comprises a microfabricated reservoir, controlled-release cover and drug formulations, which were made of photopolymeized tri(ethyleneglycol)dimethacrylate (TEGDM) and poly(ethyleneglycol)dimethacrylate (PEGDM). Here, we show that the release of multiple drugs can be tuned by changing the formulations of the drug as well as the covering, and demonstrate the transport of drugs into the ocular tissue in rats using fluorescents.

2. Materials and methods

2.1. Materials

PEGDM (*Mn* 750), TEGDM (*Mw* 286.3) and 2-hydroxy-2-methylpropiophenone were purchased from Aldrich (USA). Polydimethylsiloxane (PDMS), fluorescein (FL, *Mw* 332.31), rhodamine-B (Rho, *Mw* 479.02) and 4,6-diamidino-2-phenylindole dihydrochloride (DAPI, *Mw* 350.25) were purchased from Wako (Japan).

2.2. Device fabrication

The device consists of a reservoir that can contain different types of sustained release formulations and is sealed with a controlled release cover (Fig. 1c). PEGDM and TEGDM including 1% 2-hydroxy-2-methylpropiophenone as a photoinitiator were used for device materials. For the preparation of the reservoir, TEGDM prepolymer was poured into the PDMS mold fabricated via a microfabrication technique using a microprocessing machine (MicroMC-2, PMT Co.) (Supplementary Fig. S.1), and photopolymerized for 3 min with UV light (HLR400F-22, Sen Lights) at an intensity of 7.4 mW cm^{-2}. After loading the drugs, a reservoir cover was prepared by applying a prepolymer mixture of the required concentrations of PEGDM and TEGDM to the reservoir, followed by UV curing for 3 min. For the preparation of the fluorescent formulations, the fluorescents were combined with a mixture of a predetermined ratio of PEGDM and TEGDM and poured into PDMS molds and photopolymerized for 3 min. All fluorescent formulations had a fluorescent concentration of 50 mg ml^{-1} and the volume was 1.2 μl (60 μg) or 0.4 μl (20 μg) for single-fluorescent delivery or multi-fluorescent delivery devices, respectively. The dimensions of the device were 2 mm × 2 mm × 1 mm (external) and 1.55 mm × 1.55 mm × 0.5 mm (internal; maximum loading volume, 1.2 μl). PEGDM/TEGDM prepolymer mixture ratios of 100%/0%, 80%/20%, 60%/40%, 40%/60%, 20%/80% and 0%/100% were designated as P100, P80, P60, P40, P20 and P0, respectively.

2.3. Characterization of diffusion mechanism through the PEGDM/TEGDM system

The permeability of FL in phosphate-buffered saline (PBS) (0.5 mg ml^{-1}, 20 μl) through the PEGDM/TEGDM reservoir (4 mm × 4 mm × 1.5 mm, internal) was assessed by monitoring the increase in fluorescence in the external PBS (1 ml) solution with time ($n = 5$). To characterize the diffusion mechanism through the PEGDM/TEGDM system, we determined the swelling ability of the PEGDM/TEGDM polymers. The samples (size: 5 mm × 5 mm × 2 mm) with various PEGDM/TEGDM ratios were weighed in air before (W_b) and after (W_a) immersion for 24 h in 10 ml of PBS, and the swelling ratio ($W_a/W_b \times 100$) was calculated ($n = 5$).

2.4. In vitro release study

For the single delivery study, FL was pelletized with P60 and loaded in the device, followed by sealing with P100, P60 or P40 covers. For the multiple delivery, three types of fluorescents, FL, Rho and DAPI, were pelletized each with different ratios of PEGDM/TEGDM and loaded in the device, followed by sealing with P100 or P60 covers. The devices were each incubated in 1 ml of PBS at 37 °C. To estimate the amounts of fluorescent that had diffused out of the devices, the fluorescence intensities of the PBS solutions

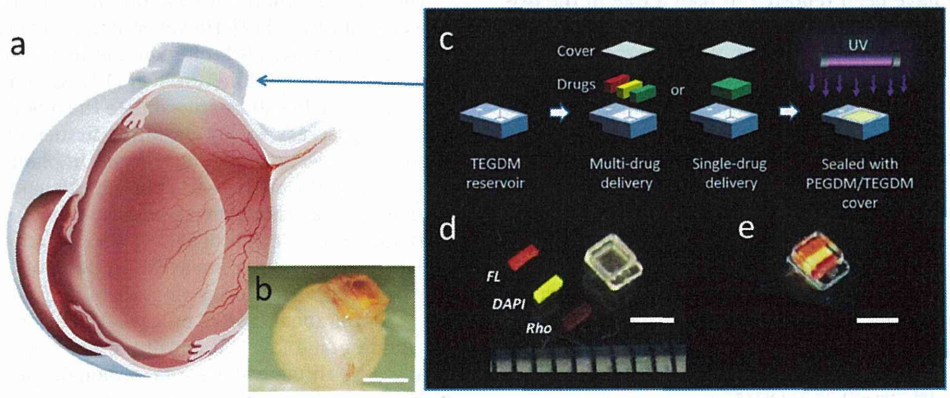

Fig. 1. (a) Schematic image of transscleral intraocular multi-drug delivery using a polymeric device placed on the sclera. (b) Photograph of the rat eye where the device was implanted on the sclera for 3 days. (c) Image shows assembling process of the device that consists of three kinds of fluorescents pelletized with PEGDM/TEGDM, a reservoir made of TEGDM and a controlled release cover made of PEGDM/TEGDM. After loading the pellets in the reservoir, the cover was sealed on the reservoir by UV curing. (d) Photographs showing three kinds of fluorescent pellets, including FL, Rho and DAPI, and a reservoir before assembling, and (e) the device after assembling. Scale bars, 2 mm.

were measured spectrofluorometrically (FluoroscanAscent; Thermo), where fluorescence excitation (ex) and emission (em) for FL, Rho and DAPI was measured at ex. 485 nm/em. 538 nm, ex. 544 nm/em. 590 nm and ex. 355 nm/em. 460 nm, respectively ($n = 6$). The PBS was replenished during the course of the release study to ensure that the concentration of fluorescent molecules was below 20% of its saturation value at all times. The results were expressed as amount determined using a standard curve.

2.5. Animal experiments

Male Sprague–Dawley rats (SLC) weighing 250–300 g were used in this study. All animals were handled in accordance with the Association for Research in Vision and Ophthalmology Statement for the Use of Animals in Ophthalmic and Vision Research after receiving approval from the Institutional Animal Care and Use Committee of the Tohoku University Environmental & Safety Committee (No. 2013MdA-218).

2.6. Implantation

The rats were anesthetized with ketamine hydrochloride (90 mg kg^{-1}) and xylazine hydrochloride (10 mg kg^{-1}). Their ocular surfaces were anesthetized with a topical instillation of 0.4% oxybuprocaine hydrochloride. A paralimbal conjunctival incision was made 1 mm from the temporal limbus. The devices were placed onto the left eyes at the sclerae. The right eyes served as controls.

2.7. In vivo release study

After implantation, the eyes were enucleated and the conjunctiva, muscle, optic nerve and the device were carefully removed. Fluorescent images were captured using a hand-held retinal camera for fluorescein angiography (Genesis-D, Kowa) to document the fluorescence distributions around the implantation site. After taking the image, the eyes were carefully separated into the retina, vitreous, lens, cornea and sclera/choroid/retinal pigment epithelium (RPE). The retina and sclera/choroid/RPE were homogenized in 100 μl of lysis buffer (1% Triton X-100 in PBS). The homogenates were centrifuged at 15,000*g* for 10 min, and the fluorescence intensity of the 80 μl of supernatant was measured spectrofluorometrically (FluoroscanAscent) ($n = 6$). For histological examination, the eyes were frozen in liquid nitrogen. A suture was placed as a landmark at the implant site of the device. After mounting the cryostat sections in a medium (Vectashield, Vector Lab), the distribution of fluorescein was observed by fluorescent microscopy (DMI6000B, Leica).

2.8. Statistical analysis

Experimental data are presented as means ± standard deviations (SD). Statistical significance was calculated with Ekuseru-Toukei 2012 (Social Survey Research Information), using the unpaired *t*-test for normally distributed isolated pairs, and the analysis of variance (ANOVA) with Tukey's test for multiple comparisons. Differences were considered significant if $p < 0.05$ (*).

3. Results

3.1. Device fabrication

The device consists of a separately fabricated TEGDM reservoir, fluorescent formulations and a PEGDM/TEGDM cover (Fig. 1c). The device was designed to deliver various formulations and dosages. In this study, sustained-release fluorescent formulations, including a single FL pellet or multiple FL/Rho/DAPI pellets (Fig. 1d), were encapsulated in the reservoir using a cover to prolong fluorescent release by limiting the rate of fluorescent dissolution within the reservoir. After loading the fluorescent pellets, the PEGDM/TEGDM prepolymer was cast over the reservoir and UV-cured to provide a seal (Fig. 1e). Because photopolymerized TEGDM is impermeable to small molecules (see below), the reservoir is a barrier that forces unidirectional fluorescent release to the sclera side.

3.2. Diffusion mechanism through the PEGDM/TEGDM system

Fig. 2a shows that the release of FL was dependent on the PEGDM/TEGDM ratio. Pure PEGDM (P100) shows the highest permeability, whereas pure TEGDM (P0) was impermeable. The release rate estimated from the slope of the curve at the initial linear state was 1296 (P100), 684 (P80), 333 (P60), 83 (P40), 35 (P20) and 0 (P0) ng day^{-1}. The release rate gradually decreased as the cumulative release approached the plateau level (10 μg ml^{-1}, maximum concentration when FL was fully released in PBS), as was seen in P100 and P80. Fig. 2b shows that the swelling ratio increased with increasing the PEGDM ratio. Fig. 2c shows the correlation of the swelling ratio, obtained from the results in Fig. 2b, with the slope obtained from the release profile results in Fig. 2a. The correlation coefficient was 0.9904, indicating almost linear correlation between the swelling ratio and release rate.

3.3. Single FL release study

Fig. 3a shows the single release profiles of FL-loaded devices that were sealed with different types of covers. Although FL-pellets without reservoir or cover showed a rapid burst-like release over 5 days, the covered devices showed a zero-order release without an initial burst. The release rate decreased with decreasing PEGDM ratio in the cover. The release rate estimated from the gradient curve for pellet, P100-, P60- and P40-covered devices were 20.7, 1.13, 0.53 and 0.10 μg day^{-1}, respectively. The results demonstrate the ability to control the release rate from a device by changing the ratio of PEGDM/TEGDM in the cover.

Devices containing FL pellet (F60) and sealed with P100, P60 and P40 covers, and pellets without reservoir or cover, were implanted onto the sclerae of rats. The devices remained at the implantation site during the experiments and were easily removed from the implantation site at the end of experiments. Routine ophthalmological examinations showed no device-related toxic effects. To demonstrate the controllability of the in vivo release of FL, images of fluorescence in the sclera after removing the device were captured by a hand-held camera (Fig. 3b). White areas corresponding to fluorescence indicate the distribution of released FL. For the pellet only, little fluorescence was observed at 1 week after implantation, probably due to the burst-like release within 5 days. For the P100-cover devices, the intensity was high at 1 week, then decreased gradually during the subsequent 3 weeks. For the P60-cover devices, the intensity was moderate for 2 weeks, then weak intensity was sustained during the remaining 2 weeks. For the P40-cover devices, weak fluorescence was sustained during 4 weeks. Trends in the fluorescence intensity were almost comparable to the in vitro release results (Fig. 3a).

Fig. 4a–d shows sectional images of an eye around the implantation site. FL (green areas) penetrated the sclera at least 1 day after implantation (Fig. 4a and c), and then reached the choroid/RPE at least 3 days after implantation (Fig. 4b and d). Intense fluorescent can be seen at the RPE, one of the blood–retinal barriers (Fig. 4d). Blurred fluorescent that passed through the RPE can be seen at the retina, indicating the passing of the molecules through the RPE into the neural retina. The amount of FL in the

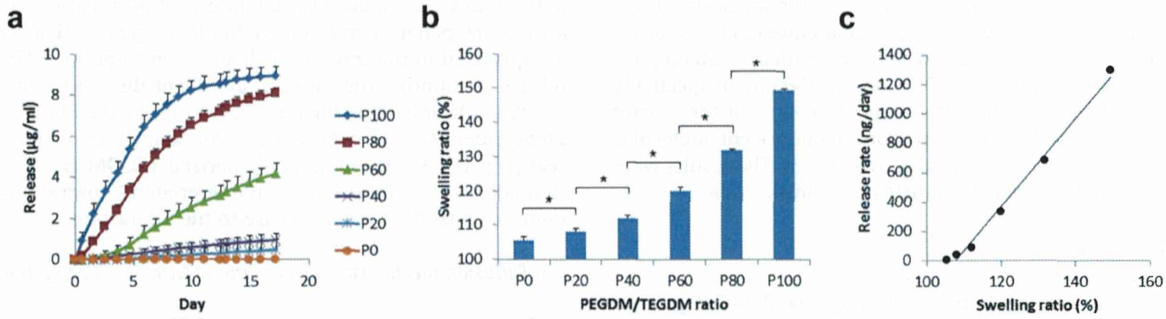

Fig. 2. (a) Permeability of FL in PBS through the PEGDM/TEGDM reservoir with various PEGDM/TEGDM ratios. The release was assessed by monitoring the increase in fluorescence in the external PBS solution with time. (b) Swelling ability in PBS of PEGDM/TEGDM polymers (size: 5 mm × 5 mm × 2 mm) with various PEGDM/TEGDM ratios. (c) Correlation between swelling ratio in (b) and release rate. Release rate was estimated from the slope of the curve of the line at the initial stable release period in (a). Values are mean ± SD. $^*p < 0.05$ (one-way analysis of variance (ANOVA) with Tukey's test).

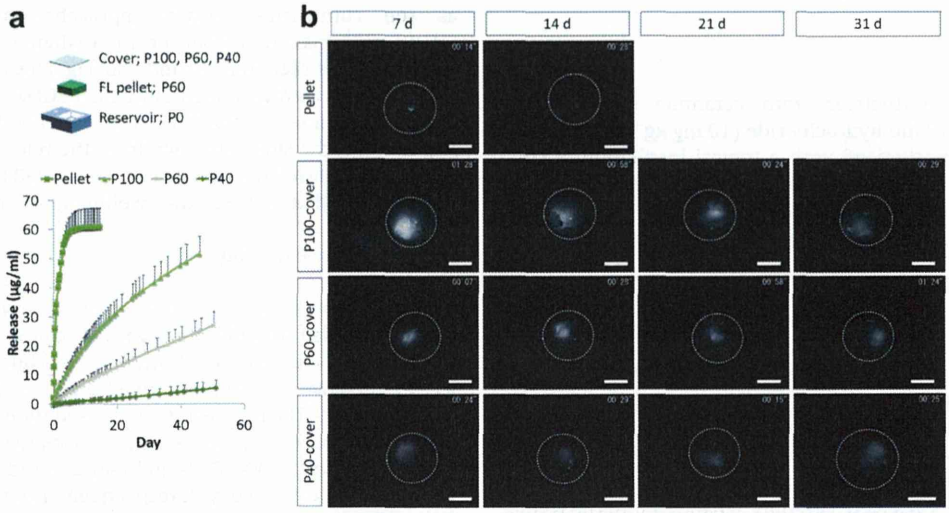

Fig. 3. (a) Release profiles of a single-drug delivery device that consists of a FL formulation pelletized with P60 and various types of cover (P100, P60 and P40), and FL pellet with no reservoir or cover. FL release was monitored spectrofluorometrically. (b) Fluorescent images of the sclera after removing the devices. Devices were implanted on the sclerae in rats for 7, 14, 21 and 31 days. White areas show released FL and circular dotted lines show the shape of the eyeball. Values are mean ± SD. Scale bars: 2 mm.

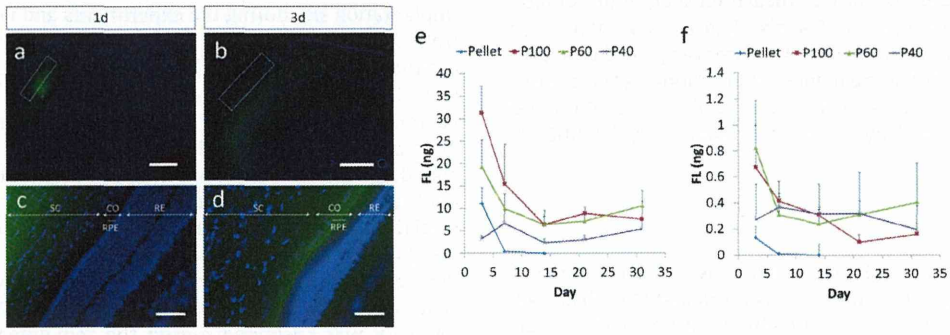

Fig. 4. The distribution of FL (green) in the retina and sclera around the implantation site (a, c) 1 day and (b, d) 3 days after implantation (square dots: device implantation site). Cell nuclei were stained with DAPI (blue). FL accumulated at RPE by day 3 after implantation and a portion of FL penetrated through the RPE and reached the retina. The amounts of FL in the sclera/choroid/RPE (e) and retinal fractions (f) during 1 month implantation. Abbreviations: sclera (SC), retinal pigment epithelium (RPE), choroid (CO) and retina (RE). Scale bars: 1 mm (a, b), 100 μm (c, d). Values are mean ± SD.

sclera/choroid/RPE, and retinal fractions during 4 weeks' implantation was measured. For the sclera/choroid/RPE fraction (Fig. 4e), the amount of FL correlated with the release profiles of the covered devices at the first week (P100 > P60 > P40). Pellet only showed almost no fluorescence after 1 week due to the burst-like release within 5 days, as is seen in Fig. 3a. From 2 weeks' implantation onwards, the amounts of FL for the P100- and P60-covered devices were at almost the same level, whereas the amount for the P40-covered device was consistently at a lower level during the successive incubation. These results are well matched with the fluorescent images on the sclera shown in Fig. 3b. For the retinal fraction (Fig. 4f), the amount of FL differed among the devices

for the first week, but was then maintained at almost the same level for each device during the following 2 weeks. Pellet only was unable to deliver FL to the retina except during the early days. After 3 weeks, the FL level for the P100-covered device was lower, while the level for the P40-covered device had decreased after 4 weeks. Although the amount of FL in the retina shows little correlation with the release profiles, the results demonstrate that fluorescent molecules released from the devices could reach the retina during the 4 weeks of implantation and the amount of FL was reduced to between 1/30 and 1/40 at the retina after passing through the sclera.

3.4. Multiple FL/Rho/DAPI release study

The simultaneous independently controlled multiple release was tested using three kinds of fluorescents, FL, Rho, and DAPI, which may mimic low-molecular-weight drugs. The device was filled with three kinds of pellets, each with different ratios of PEGDM/TEGDM. The release profiles of each pellet are shown in Supplementary Fig. S.2. DAPI pelletized with P100 (D100) was always included in the device as a constant control. FL was pelletized with P100 (F100), P70 (F70) and P60 (F60). Rho was also pelletized with P100 (R100), P70 (R70) and P60 (R60). Fig. 5a–c shows that the release rate of the molecules can be tuned by changing the composition of each pellet. For example, the release rate of FL or Rho varied as the PEGDM ratio changed (Fig. 5a vs. Fig. 5b), whereas that of DAPI was constant. When the device was sealed with a P60 cover, the absolute amount released decreased to between one-fourth and one-eighth in all of the devices compared to the P100-covered devices, but importantly, the ability to independently control the release rates of the molecules was maintained (Fig. 5d–f). If the release results were sorted for each molecule, the release kinetics of each molecule was always dependent on the PEGDM/TEGDM ratio of the pellet (Supplementary Fig. S.3). These results indicate that the release kinetics can be tuned via two independent diffusion mechanisms afforded by a sustained-release formulation and a controlled release cover.

Devices containing a combination of F60/R40/D60 pellets (device A) or F60/R60/D40 pellets (device B), sealed with a P60 cover, were implanted onto the rat sclerae. Fig. 6a–h shows the sectional images for 1 and 4 weeks after implantation. Magnified images showed fluorescence at the outer nuclear layer (ONL) in the retina and the intensity of the fluorescence correlates with device condition; device A, which releases DAPI at a faster rate than device B, shows more intense blue fluorescence in the ONL compared with device B (Fig. 6b and f). On the other hand, device B, which releases Rho at a faster rate than device A, exhibits more red fluorescence in the retina than that of device A (Fig. 6d and h). Low magnification images of the sections showed the local distribution of released fluorescents around the implantation site 1 and even 4 weeks after implantation (Fig. 6a, c, e and g). This may indicate that the released drug is specifically delivered to the retina local to the implantation site.

The amounts of fluorescence in the sclera/choroid/RPE (Fig. 7a–c) and the retina fractions (Fig. 7d–f) at 1, 2 and 4 weeks after implantation were measured. Because FL was set to release at the same rate in each device, there was no significant difference between the amount of FL detected in the fractions for device A or B (Fig. 7a and d). On the other hand, the amount of Rho in sclera/choroid/RPE and retinal fractions for device B was higher than for device A, and at 4 weeks' implantation a significant difference (p value: 0.042) can be seen in the sclera/choroid/RPE fraction (Fig. 7b). Similarly, the amount of DAPI for device A was significantly higher than for device B at 4 weeks' implantation (p value; 0.037) (Fig. 7c). There was no difference between Rho and DAPI intensities in the retina for the devices (Fig. 7e and f).

4. Discussion

We established a transscleral multi-drug delivery device with which we demonstrated the transport of low-molecular-weight compounds into the ocular tissue using fluorescents. The release of multiple drugs can be tuned by changing the formulations of the drug as well as the covering. The ability to control the release of fluorescents from the PEGDM/TEGDM system may be explained by the results of swelling tests (Fig. 2). The polymers made of short chains of TEGDM are likely to be compact, with little ability to swell, and impermeable to low-molecular-weight compounds. On the other hand, long chains of PEGDM may result in more open polymer networks, showing a greater tendency to swell, facilitating permeation of small molecules. Further, the release rate of each fluorescent differs, even when we used the same pelletized

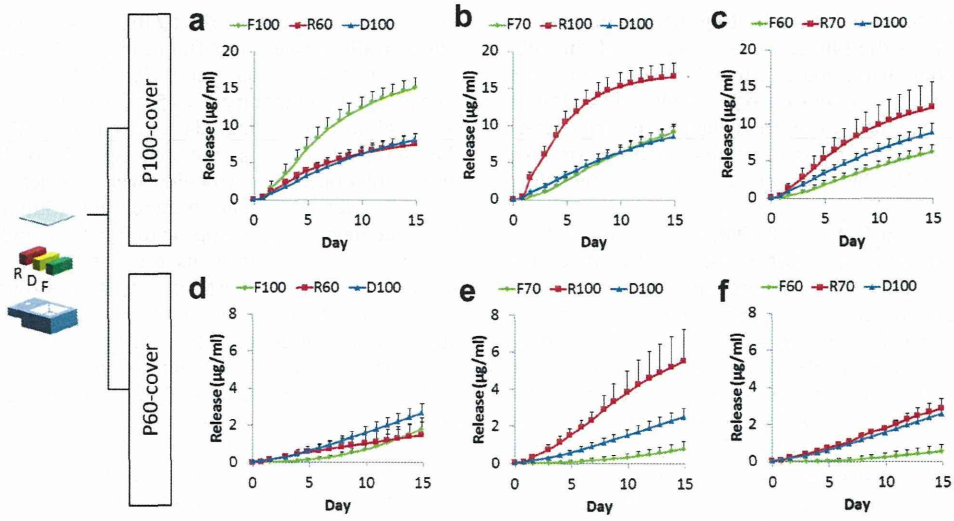

Fig. 5. (a–f) Release profiles of a multi-drug delivery device that consists of three types of fluorescent pellets (FL, Rho and DAPI, designated F, R and D, respectively, in the schematic) made of various PEGDM/TEGDM content, and two types of cover (P100 cover: (a–c), P60 cover: (d–f)). DAPI was pelletized with P100 as a constant release control. FL and Rho were pelletized with P100, P70 and P60, respectively. Values are mean ± SD.